Kinetics of Furan Formation from Ascorbic Acid during Heating under Reducing and Oxidizing Conditions

Burçe Ataç Mogol and Vural Gökmen*

Department of Food Engineering, Hacettepe University, 06800 Beytepe, Ankara, Turkey

ABSTRACT: This study aimed to investigate the effect of oxidizing and reducing agents on the formation of furan through ascorbic acid (AA) degradation during heating at elevated temperatures (≥ 100 °C) under low moisture conditions. To obtain these conditions, oxidizing agent, ferric chloride (Fe), or reducing agent, cysteine (Cys), was added to reaction medium. Kinetic constants, estimated by multiresponse modeling, stated that adding Fe significantly increased furan formation rate constant, namely 369-fold higher than that of control model at 100 °C. Rate-limiting step of furan formation was found as the reversible reaction step between intermediate (Int) and diketogluconic acid (DKG). Additionally, Fe decreased activation energy of AA dehydration and furan formation steps by 28.6% and 60.9%, respectively. Results of this study are important for heated foods, fortified by ferric ions and vitamins, which targets specific consumers, e.g. infant formulations.

KEYWORDS: furan, ascorbic acid, heat treatment, oxidation−reduction potential, multiresponse modeling

■ INTRODUCTION

Furan is a volatile oxygen heterocycle formed in a number of heated foods. It has received considerable attention as it is classified 'possibly carcinogenic to humans' (Group 2B) by the International Agency for Research on Cancer (IARC).[1] Moro et al.[2] reported that furan was found to induce hepatocellular adenomas and carcinomas in rats and mice and a high incidence of cholangiocarcinomas in rats at doses higher than of 2 mg per kg per body weight. Due to its low boiling point, furan, formed during thermal processing, easily vaporizes. However, this gives rise to concern in canned or jarred foods as furan accumulates in the headspace. Monitoring furan levels in foods has implications for its occurrence in a broad range of products (roasted coffee, bakery products, baby foods, etc.) from no detectable levels to 7000 μg/kg.[3−12]

Ascorbic acid (AA) has been shown as one of the major precursors of furan formed by different thermal processes.[13−16] Maga reported that the primary source of furans in food is thermal degradation of carbohydrates such as glucose, lactose, and fructose.[17] Moreover, a U.S. FDA report indicated that a variety of carbohydrate/amino acid mixtures or protein model systems (e.g., alanine, cysteine, casein) and vitamins (AA; dehydroascorbic acid, DHAA; thiamin) have been used to generate furans in food.[18] Furan could also be formed through oxidation of polyunsaturated fatty acids and carotenoids at elevated temperatures.[13] Formation of furan has been studied in simple model systems containing precursors in order to understand their contributions in the formation mechanism. In a previous study, Perez Locas and Yaylayan proposed a mechanism describing that AA might be transformed under nonoxidative pyrolytic conditions to 2-deoxyaldotetrose as a key intermediate leading directly to furan.[13]

Model systems are widely used to set experiments in order to understand the fate of reactions. However, foods are complex systems in which different constituents create different conditions for the reactions occurring in foods during thermal processing. One of these conditions to be considered is the oxidation−reduction potential of the food. In a previous study, it was reported that the oxidation−reduction potential of the reaction medium significantly affects the rate of AA degradation.[19]

On the other hand, reaction mechanisms in foods are challenging, as key compounds involve in many simultaneous and successive steps. In this sense, multiresponse modeling is a useful approach to understand such mechanisms. Multiresponse modeling, which is based on measurement of reactants and products simultaneously, provides the possibility to estimate parameters more accurately than with uniresponse modeling in which only one reactant or only one product is analyzed.[20] Modeling the formation of compounds derived from kinetic data is a great tool to estimate kinetic parameters, which facilitate to understand the reaction mechanism. Initially, a proposed reaction mechanism describing the change of concentration of key reaction compounds is needed to develop a mechanistic model.[20]

This study aimed to understand the effect of oxidizing and reducing agents on the formation of furan through AA degradation during heating at elevated temperatures (≥ 100 °C) under low moisture conditions. Ferric chloride ($FeCl_3$) or cysteine (Cys) was added to the model system to create oxidizing or reducing conditions, respectively. Both Cys and Fe^{3+} ions may be naturally present in the foods. Ferric ions might also migrate from metal containers used in processing,[14] or foods might be fortified by ferric ions and/or AA targeting specific consumers, e.g. infant formulations. Multiresponse kinetic modeling was used to obtain more information about the degradation reaction network of ascorbic acid into furan proposed previously[13] as well as to determine kinetic constants and rate limiting step.

■ MATERIALS AND METHODS

Chemicals. Solvents, HPLC-grade water, and methanol used for chromatographic analysis were purchased from Sigma-Aldrich (Steinheim, Germany), and formic acid (98%) was purchased from J.T. Baker (Deventer, Holland). L-(+)-Ascorbic acid (min. >99.7%), L-(+)dehydroascorbic acid, cysteine (min 99%), furan (99.9%), and silica gel 60GF (for thin-layer chromatography) were obtained from Merck, and Fe(III)-chloride anhydrous was obtained from Riedel-de Haën (Seelze, Germany). d_4-Furan (for NMR 99% atom) was purchased from Acros Organics (New Jersey). Stock solutions of furan and spiking d_4-furan were prepared in methanol at a concentration of 1000 mg/mL. All solutions were prepared and kept at 4 °C.

Preparation of Model Systems. Three model systems were prepared to monitor furan formation from AA under different conditions. Reaction mixtures were prepared containing 100 μmol/mL AA in water. Oxidizing or reducing agents were added to the reaction mixtures, specifically 10 μmol Fe^{3+} equivalent ferric chloride or 10 μmol Cys, respectively. A total of 100 μL of these reaction mixtures, containing 10 μmol AA, 1 μmol Fe^{3+}, or 1 μmol Cys, was mixed with 30 mg of silica gel in 20 mL headspace vials and then covered with additional 270 mg of silica gel. The vials were sealed with crimp cap, immediately, and then heated in a temperature-controlled oven (Memmert, Schwabach, Germany) at 100 °C, 120 °C, and 140 °C for 5, 10, 15, 20, 30, 60, 120, 180, and 360 min. All reactions were performed in duplicate. The reaction conditions and response variables for the model systems used for kinetic modeling are given in Table 1.

Table 1. Range of Reaction Conditions and Response Variables Used for Multiresponse Kinetic Modeling

	range of reaction conditions		
model	T (°C)	t (min)	response variables
control	100−140	0−360	furan, AA, DHAA, DKG
Fe	100−140	0−360	furan, AA, DHAA, DKG
Cys	100−140	0−360	furan, AA, DHAA, DKG

Analysis of Furan. After reaction, the vials containing reactants and reaction products were spiked through septa with 1.0 nmol of d_4-furan. Determination of furan was carried out using Agilent 6890N series GC coupled with Agilent 5973 mass selective detector. Furan was extracted by 75 mm carboxen-polydimethylsiloxane solid phase micro extraction (SPME) fiber (Supelco, Bornem, Belgium). Before use, the fiber was conditioned in the GC injection port under helium flow in accordance with the temperature and time recommended by the manufacturer. Fiber was then incubated in headspace of vials in a temperature-controlled oven at 30 °C for 30 min. The vials were gently mixed every 5 min. Thermal desorption of analytes was carried out by exposing the fiber in the GC injector port at 200 °C for 5 min, and splitless injection was used. Separation was performed on a 24 m × 0.32 μm, 20 μm HP-PLOTQ column. The MS was operated in electron ionization mode. Working conditions were as follows: injector 2 mL/min; oven temperature, 100 °C (5 min), with a temperature ramp of 10 °C/min to 200 °C and held for 15 min. The MS source temperature was 230 °C, and the MS quad temperature was 150 °C, with a dwell time of 100 ms. Furan was detected using single-ion monitoring of the fragments m/z 68 and 39. The internal standard d_4-furan was detected by monitoring the fragments m/z 72 and 42. The concentration of furan in the reaction mixtures was calculated by means of a calibration curve built in a range of 0−15 nmol (0, 0.01, 0.15, 1.5, 3.0, 7.5, 15.0 nmol). The limit of quantification was 0.01 nmol per reaction mixture for furan under the stated analytical conditions. All analytical determinations were performed in duplicates.

Analysis of AA, DHAA, and Reaction Intermediates by High-Resolution Mass Spectrometer. AA, DHAA, and other intermediates were extracted by adding 5 mL of 10 mM formic acid in water to vial in two steps (2 × 2.5 mL). After mixing thoroughly, the extracts were transferred to tube, which was then centrifuged at 5000g for 10 min. Supernatants were filtered through 0.45 μm nylon filter to HPLC vials.

An ultra high-performance liquid chromatography (U-HPLC) Accela system (Thermo Fisher Scientific, San Jose, CA) consisting of a degasser, a quaternary pump, an auto sampler, and a column oven was used. The U-HPLC was directly interfaced to an Exactive Orbitrap MS (Thermo Fisher Scientific, San Jose, CA). Chromatographic separations were performed on a HIBAR Purospher-STAR RP-18e column (150 × 4.6 mm, 5 μm particle size) (Merck, Darmstadt, Germany). An isocratic mixture (95:5, v/v) of 0.1% formic acid in water and 0.1% formic acid in methanol was used as the mobile phase at a flow rate of 500 μL/min at 30 °C. The total run time was 10 min. The Exactive Orbitrap MS equipped with a heated electrospray interface was operated in the negative mode, scanning the ions in m/z range of 50−300. The resolving power was set to 100 000 full width at half-maximum resulting in a scan time of 0.5 s. Automatic gain control target was set into balanced; maximum injection time was 50 ms. The interface parameters were as follows: the spray voltage of 4 kV, the capillary voltage of 25 V, the capillary temperature of 350 °C, a sheath gas flow of 45, and auxiliary gas flow of 20. The instrument was externally calibrated by infusion of a calibration solution (m/z 138 to m/z 1822) by means of an automatic syringe injector (Chemyx Inc. Fusion 100 T, U.S.A.). The calibration solution (Sigma-Aldrich) contained caffeine, Met-Arg-Phe-Ala, Ultramark 1621, and acetic acid in the mixture of acetonitrile/methanol/water (2:1:1, v/v/v). Data were recorded using Xcalibur software version 2.1.0.1140 (Thermo Fisher Scientific). The concentrations of AA and DHAA in the reaction mixtures were calculated by means of calibration curves (0.0, 0.05, 0.10, 0.25, 0.50, 1.0 μmol). All analytical determinations were performed in duplicates.

Statistical Analysis. Data were analyzed by one-way analysis of variance (ANOVA) using Duncan test with the SPSS program (SPSS 16.0). Significance was defined as $p < 0.05$.
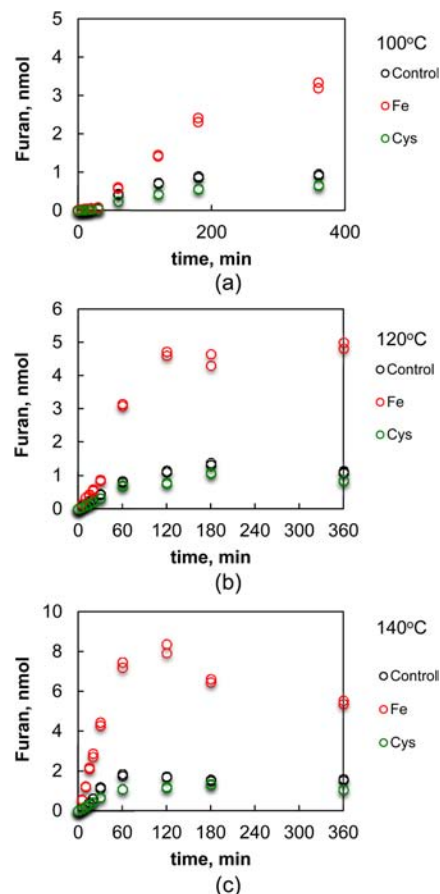

Figure 1. Amount of furan formed in different model systems (control, Fe, Cys) during heating at different temperatures: (a) 100 °C, (b) 120 °C, (c) 140 °C.
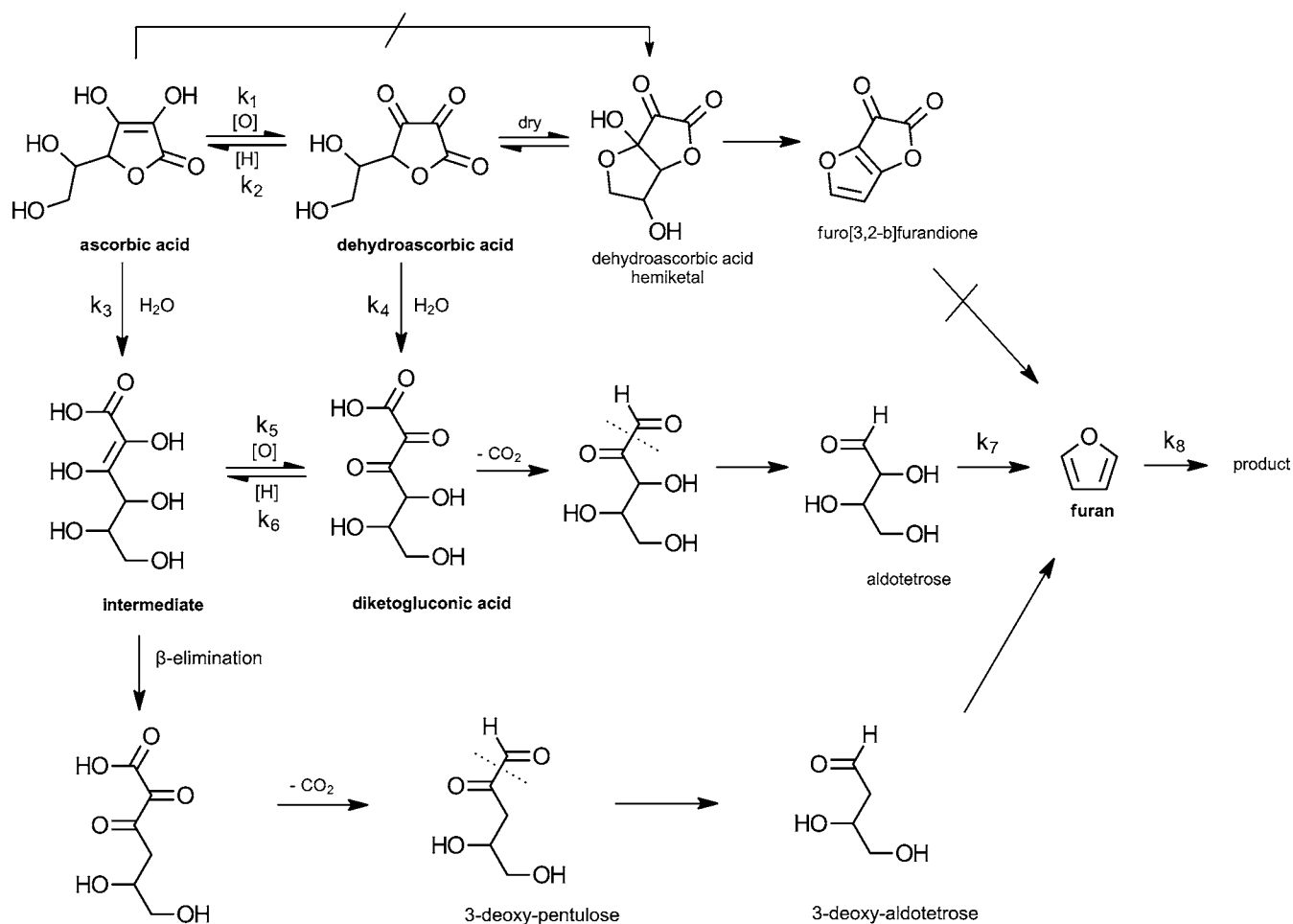
Figure 2. Mechanism of furan formation from AA adapted from Perez Locas and Yaylayan.[13] Compounds indicated in bold were used as response variables in multiresponse kinetic modeling. [O]: oxidation, [H]: reduction.

■ RESULTS AND DISCUSSION

Changes in furan concentrations in three models (control, Fe, and Cys) were given in Figure 1 indicating that presence of reducing or oxidizing agents in the reaction medium affected furan formation. Adding ferric chloride to the model significantly accelerated furan formation from AA during heating at temperatures exceeding 100 °C ($p < 0.05$). On the other hand, presence of Cys did not have significant effect on furan formation ($p > 0.05$).

Figure 1 also shows that increasing temperature increased furan concentration regardless of the composition of reaction medium. Likewise, reaction time also showed effect on furan formation. Increased thermal load, either increasing temperature or time, also increased the amount of furan formed to a certain extend. At 100 and 120 °C, furan concentration reached to a steady apparent maximum. However, at 140 °C, furan concentration after reaching to its apparent maximum level within 2 h of heating began to decrease slightly in the presence of ferric chloride. This could be the result of increased furan degradation rate, which becomes higher than its formation rate at those conditions.

In this study, furan formation was modeled using multiresponse approach from the kinetic data obtained at different temperatures using Athena Visual Studio software (Version 14.2). The mechanism of furan formation from AA proposed by Perez Locas and Yaylayan[13] was used for this purpose. The reaction

network shown in Figure 2 is a representation of the possible oxidative and nonoxidative degradation pathways. Among these pathways, some were selected to simplify the reaction network for modeling purposes. Such selections were based on experimental measurements of the reactants and certain products (compounds indicated in bold). The proposed mechanism was slightly modified by adding a reversible reduction step to oxidation of Int to diketogluconic acid (DKG). The reason was a reduction step could take place, if there would be an oxidation step in these model systems having different oxidation–reduction conditions.

The model was formed with differential eqs 1, 2, 3, 4, 5, and 6 which were derived according to the proposed mechanism. The model was then fitted to experimental data, and rate constants (k_1 to k_8) were estimated for each model system and temperature. The proposed model successfully described the experimental data, as given in the example in Figure 3.

$$\frac{d[AA]}{dt} = -k_1[AA] - k_3[AA] + k_2[DHAA] \tag{1}$$

$$\frac{d[DHAA]}{dt} = k_1[AA] - k_2[DHAA] - k_4[DHAA] \tag{2}$$

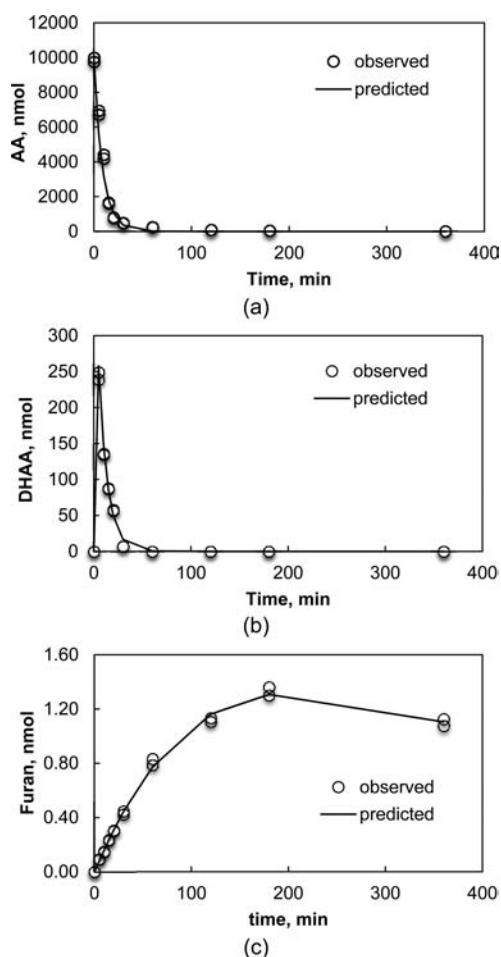$$\frac{d[Int]}{dt} = k_3[AA] - k_5[Int] + k_6[DKG] \tag{3}$$

Figure 3. Change of the amounts of AA, DHAA, and furan with time in the model system (control) during heating at 120 °C (solid lines indicate model fit).

$$\frac{d[DKG]}{dt} = k_4[DHAA] + k_5[Int] - k_6[DKG] - k_7[DKG] \tag{4}$$

$$\frac{d[furan]}{dt} = k_7[DKG] - k_8[furan] \tag{5}$$

$$\frac{d[product]}{dt} = k_8[furan] \tag{6}$$

The rate constants for the degradation of AA to Int (k_3), and the formation of furan (k_7) are given in Table 2. Adding ferric chloride significantly increased furan formation rate constant at all temperatures, while adding Cys significantly decreased ($p < 0.05$). Moreover, k_7 increased with the increase of temperature in control and Cys containing model systems. Rate constant of the degradation of AA to Int was higher than that of AA to DHAA. For example, k_1 and k_3 for the control model system heated at 140 °C were calculated as 0.042 min^{-1} and 0.182 min^{-1}, respectively. Rate constant of the degradation of AA to Int (k_3) increased in the presence of ferric chloride or as heating temperature increased. Cys had no significant effect on this reaction ($p > 0.05$) at any temperatures.

High-resolution MS offers advantages to help identify the structure of compounds in complex reaction systems. In this study, formation of reaction intermediates, proposed by Perez Locas and Yaylayan,[13] were confirmed by high resolution MS.

Table 2. Rate Constants Calculated for the Degradation of AA to Int (k_3) and the Formation of Furan (k_7)[a]

T (°C)	model	k_3, min^{-1}	k_7, min^{-1}
100	control	$5.34 \times 10^{-02} \pm 2.98 \times 10^{-03a}$	$2.13 \times 10^{-05} \pm 8.71 \times 10^{-06a}$
	Fe	$2.69 \times 10^{-01} \pm 2.52 \times 10^{-02b}$	$7.86 \times 10^{-03} \pm 2.16 \times 10^{-03b}$
	Cys	$5.77 \times 10^{-02} \pm 6.17 \times 10^{-03a}$	$7.99 \times 10^{-07} \pm 1.08 \times 10^{-07a}$
120	control	$1.10 \times 10^{-01} \pm 4.72 \times 10^{-03a}$	$5.58 \times 10^{-03} \pm 7.56 \times 10^{-04a}$
	Fe	$4.15 \times 10^{-01} \pm 5.38 \times 10^{-02b}$	$2.97 \times 10^{-02} \pm 5.93 \times 10^{-03b}$
	Cys	$1.04 \times 10^{-01} \pm 1.40 \times 10^{-02a}$	$2.14 \times 10^{-05} \pm 4.38 \times 10^{-06a}$
140	control	$1.82 \times 10^{-01} \pm 1.52 \times 10^{-02a}$	$4.22 \times 10^{-02} \pm 2.60 \times 10^{-02a,b}$
	Fe	$6.47 \times 10^{-01} \pm 1.09 \times 10^{-01b}$	$1.58 \times 10^{-01} \pm 4.71 \times 10^{-02b}$
	Cys	$2.04 \times 10^{-01} \pm 3.56 \times 10^{-02a}$	$3.85 \times 10^{-04} \pm 9.37 \times 10^{-05a}$

[a]Different letters indicate statistically significant differences ($p < 0.05$) for the rate constants calculated for control, Cys and Fe models at different temperatures.

Two compounds in this reaction scheme, [Int]$^-$ (m/z 193) and [DKG]$^-$ (m/z 191), were successfully extracted from the total ion chromatograms. As they could not be quantified, peak areas were considered to compare as given in Table 3.

Table 3. Effects of Oxidizing and Reducing Agents on the Formation of Int and DKG during Heating the Models Systems Containing AA at Different Temperatures for 5 Minutes[a]

T (°C)	model	peak area	
		Int m/z 193	DKG m/z 191
100	control	ND[b]	ND
	Fe	$5.21 \times 10^4 \pm 3.42 \times 10^3$	$1.13 \times 10^4 \pm 6.50 \times 10^2$
	Cys	ND	ND
120	control	$1.31 \times 10^4 \pm 7.46 \times 10^2$	$6.45 \times 10^3 \pm 3.38 \times 10^2$
	Fe	$1.22 \times 10^5 \pm 9.36 \times 10^3$	$4.12 \times 10^4 \pm 2.48 \times 10^3$
	Cys	$0.62 \times 10^4 \pm 3.51 \times 10^2$	$3.14 \times 10^3 \pm 2.23 \times 10^2$
140	control	$2.18 \times 10^4 \pm 1.40 \times 10^3$	$1.00 \times 10^4 \pm 6.88 \times 10^2$
	Fe	$1.17 \times 10^5 \pm 7.70 \times 10^3$	$7.87 \times 10^4 \pm 3.93 \times 10^3$
	Cys	$1.43 \times 10^4 \pm 8.98 \times 10^2$	$7.50 \times 10^3 \pm 7.05 \times 10^2$

[a]Signal intensities are given as peak area of corresponding compounds detected by high resolution MS. [b]ND: Not detected.

Results showed that presence of ferric chloride promoted the formation of both intermediates. Although there was no formation of Int and DKG in control and Cys models heated at 100 °C for 5 min, presence of ferric chloride induced both compounds to be formed. Peak area of Int was found to be higher than DKG at all temperatures, indicating that the main reaction pathway to form furan was through Int formed from AA. As discussed above, presence of Cys significantly decreased furan formation rate constant (k_7), however furan concentration was not affected equally. On the basis of these results it could be concluded that the rate-limiting step of the furan formation reaction mechanism was the reversible reaction step between Int and DKG.

The results of the present study revealed that furan formation was strongly affected by ferric chloride. However, Becalski and Seaman was reported that adding ferric chloride to the AA model did not increase furan formation in their model system.[14] This conflict may result from the differences in the reactants' concentration or in the state of the model system. They used a relatively low amount of ferric chloride compared with AA (approximately 50 μmol AA and 0.062 μmol FeCl$_3$) in aqueous model system, while we used 10 μmol AA and 1 μmol Fe^{3+} in the low moisture model system.

Temperature dependence of simple chemical reactions was empirically described by Arrhenius' law, which is expressed as

$$k = A \exp\left(-\frac{E_a}{RT}\right) \qquad (7)$$

in which k (s^{-1}) is the reaction rate constant, A (s^{-1}) is a pre-exponential factor, E_a is the activation energy (J mol^{-1}), R (1.987 J mol^{-1} K^{-1}) is the gas constant, and T (K) is the absolute temperature. The Arrhenius' equation gives a quantitative account.[21] In the present study, linear Arrhenius dependence was obtained for the degradation of AA to Int (k_3), and the formation of furan (k_7) (Figure 4). For k_3, the activation energies were
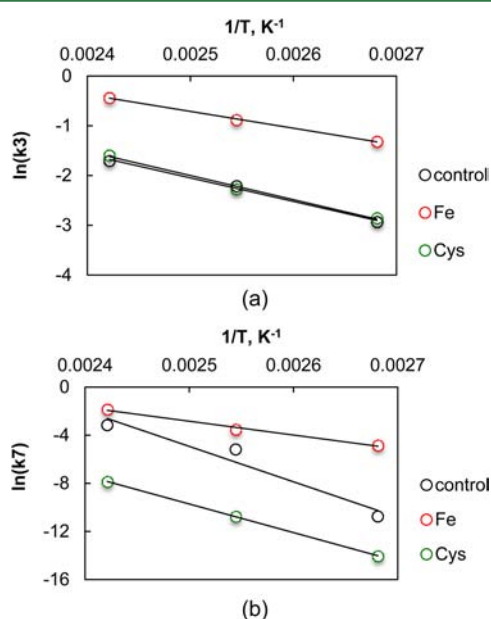

Figure 4. Arrhenius plots for (a) the degradation of AA into Int (k_3), and (b) the formation of furan (k_7).

calculated as 39.40, 28.14, and 40.28 kJ mol^{-1} for control, Fe, and Cys models, respectively. Moreover the activation energies for k_7 were calculated as 244.93, 95.79, and 197.95 kJ mol^{-1} for control, Fe, and Cys models, respectively. It is clear that both reaction steps were affected by ferric chloride in terms of decreasing activation energy, which means that reactants need less energy to start the reaction and carry on spontaneously. Furthermore, it was previously reported that activation energy of the degradation of AA ranges between 20 to 167 kJ mol^{-1} in aqueous systems, which is comparable with the results of this study.[22]

Composition of food is important, as it constitutes the reaction medium. Each constituent might affect the reactions occurring in foods during heating. As a conclusion, oxidation–reduction potential was found to be one of the main intrinsic factors to consider for furan formation through the degradation of AA. The results are considered to be relevant for low moisture foods like infant biscuits enriched with vitamins and minerals including AA and Fe^{3+}.

AUTHOR INFORMATION

Corresponding Author
*Phone: +903122977108. Fax: +903122992123. E-mail: vgokmen@hacettepe.edu.tr.

ABBREVIATIONS USED

AA, ascorbic acid; ANOVA, analysis of variance; Fe, ferric chloride; Cys, cysteine; DHAA, dehydroascorbic acid; DKG, diketogluconic acid; Int, intermediate compound; MS, mass spectrometry; SPME, solid phase micro extraction; U-HPLC, ultra high-performance liquid chromatography

REFERENCES

(1) *IARC Monographs*; International Agency for Research on Cancer (IARC): 1995.
(2) Moro, S.; Chipman, J. K.; Wegener, J. W.; Hamberger, C.; Dekant, W.; Mally, A. Furan in heat-treated foods: Formation, exposure, toxicity, and aspects of risk assessment. *Mol. Nutr. Food Res.* **2012**, *56*, 1197−1211.
(3) Hasnip, S.; Crews, C.; Castle, L. Some factors affecting the formation of furan in heated foods. *Food Addit. Contam.* **2006**, *23*, 219−227.
(4) Guenther, H.; Hoenicke, K.; Biesterveld, S.; Gerhard-Rieben, E.; Lantz, I. Furan in coffee: Pilot studies on formation during roasting and losses during production steps and consumer handling. *Food Addit. Contam. A* **2010**, *27*, 283−290.
(5) Van Lancker, F.; Adams, A.; Owczarek, A.; De Meulenaer, B.; De Kimpe, N. Impact of various food ingredients on the retention of furan in foods. *Mol. Nutr. Food Res.* **2009**, *53*, 1505−1511.
(6) Zoller, O.; Sager, F.; Reinhard, H. Furan in food: Headspace method and product survey. *Food Addit. Contam.* **2007**, *24*, 91−107.
(7) EFSA. Update of results on the monitoring of furan levels in food. *EFSA J.* **2010**, *8*, 1702-1720.
(8) Mariotti, M. S.; Granby, K.; Rozowski, J.; Pedreschi, F. Furan: a critical heat induced dietary contaminant. *Food Funct.* **2013**, *4*, 1001−1015.
(9) Jestoi, M.; Jarvinen, T.; Jarvenpaa, E.; Tapanainen, H.; Virtanen, S.; Peltonen, K. Furan in the baby-food samples purchased from the Finnish markets − Determination with SPME-GC-MS. *Food Chem.* **2009**, *117*, 522−528.
(10) Lachenmeier, D. W.; Maser, E.; Kuballa, T.; Reusch, H.; Kersting, M.; Alexy, U. Detailed exposure assessment of dietary furan for infants consuming commercially jarred complementary food based on data from the DONALD study. *Matern. Child Nutr.* **2012**, *8*, 390−403.
(11) Altaki, M. S.; Santos, F. J.; Galceran, M. T. Occurrence of furan in coffee from Spanish market: Contribution of brewing and roasting. *Food Chem.* **2011**, *126*, 1527−1532.
(12) Kim, T.-K.; Lee, Y.-K.; Kim, S.; Park, Y. S.; Lee, K.-G. Furan in commercially processed foods: Four-year field monitoring and risk assessment study in Korea. *J. Toxicol. Environ. Health, Part A* **2009**, *72*, 1304−1310.
(13) Perez Locas, C.; Yaylayan, V. A. Origin and mechanistic pathways of formation of the parent furan - A food toxicant. *J. Agric. Food Chem.* **2004**, *52*, 6830−6836.
(14) Becalski, A.; Seaman, S. Furan precursors in food: A model study and development of a simple headspace method for determination of furan. *J. AOAC Int.* **2005**, *88*, 102−106.
(15) Mark, J.; Pollien, P.; Lindinger, C.; Blank, I.; Mark, T. Quantitation of furan and methylfuran formed in different precursor systems by proton transfer reaction mass spectrometry. *J. Agric. Food Chem.* **2006**, *54*, 2786−2793.
(16) Fan, X. T. Formation of furan from carbohydrates and ascorbic acid following exposure to ionizing radiation and thermal processing. *J. Agric. Food Chem.* **2005**, *53*, 7826−7831.
(17) Maga, J. A. Furans in Foods. *Crit. Rev. Food Sci.* **1979**, *11*, 355−400.
(18) U.S.F.D.A, *Exploratory Data on Furan in Food*; 2004, URL (http://www.fda.gov/ohrms/dockets/ac/04/briefing/4045b2_09_furan%20data.pdf) (02.07.2013)

(19) Serpen, A.; Gokmen, V. Reversible degradation kinetics of ascorbic acid under reducing and oxidizing conditions. *Food Chem.* **2007**, *104*, 721−725.

(20) Van Boekel, M. A. J. S. Statistical aspects of kinetic modeling for food science problems. *J. Food Sci.* **1996**, *61*, 1750−3841.

(21) Van Boekel, M. A. J. S. Kinetic modeling of food quality: A critical review. *Compr. Rev. Food Sci. Food Saf.* **2008**, *7*, 144−158.

(22) Villota, R.; Hawkes, J. G.; Heldman, D. R.; Lund, D. B. Reaction kinetics in food system. *Handbook of Food Engineering*; CRC Press: Boca Raton, FL, 1992.

■ NOTE ADDED AFTER ASAP PUBLICATION

There was an error in Figure 2 in the version of this paper published October 11, 2013. The correct version published October 23, 2013.